Urban Forestry & Urban Greening 38 (2019) 11–21

Contents lists available at ScienceDirect

Urban Forestry & Urban Greening

journal homepage: www.elsevier.com/locate/ufug

Application of land use regression techniques for urban greening: An analysis of Tianjin, China

Ying Guo[a,b], Jason G. Su[b,*], Ya Dong[a], Jennifer Wolch[c]

[a] School of Architecture, Tianjin University, Tianjin, 300072, China
[b] Environmental Health Sciences, School of Public Health, University of California, Berkeley, Berkeley, CA, 94720-7360, USA
[c] College of Environmental Design, University of California, Berkeley, Berkeley, California, 94720-1820, USA

ARTICLE INFO

Keywords:
Land use regression
Geographic information systems
Object-based classification
Urban greening
Nitrogen dioxide
Tianjin

ABSTRACT

The land cover types in a 4 km by 4 km space centered around an air quality monitoring station in the city of Tianjin were classified using the e-Cognition software. We identified 23 air quality monitoring sites and their surrounding land cover types. The suitability of using land cover types to predict traffic-related air pollution Nitrogen Dioxide (NO_2) was tested through a machine learning land use regression (LUR) modeling technique. We found that vegetation was significantly but negatively associated with air pollution levels (correlation coefficient $r = -0.5$, $p < 0.01$) while highways and major roadways were positively and significantly associated with air pollution levels ($r = 0.60$, $p < 0.01$). The LUR model explained 84% of the total variance in measured NO_2 concentrations. The associations of the land cover types with NO_2 concentrations were then used in land cover retrofitting strategies to quantify the potential for reducing traffic-related air pollution. We identified that the improvements in air quality could reach 25% if specific urban greening strategies were fully implemented. The results of the study can help policy makers and environmental designers adopt effective air pollution reduction policies to improve air quality and protect public health in Tianjin and other urban regions in China.

1. Introduction

Air pollution has become a global problem and according to a report by the World Health Organization (WHO), 92% of the global population had elevated air pollution exposure based on the air quality standard proposed by WHO (World Health Organization, 2016). Air pollution is found to be associated with cardiovascular diseases, respiratory disease and diabetes (Bentayeb et al., 2015; Chen et al., 2016; Guan et al., 2016; Ma et al., 2017; Turner et al., 2017; Villeneuve et al., 2014). According to WHO, in 2012, three million people died prematurely due to air pollution (World Health Organization, 2016). The European Environment Agency estimated that the European countries alone had more than 20,000 premature deaths annually. Compared with the West, China has far worse air pollution (He et al., 2016; Li, 2016; Shostya, 2016; Song et al., 2017). According to the *2016 China Environmental State Bulletin* published by the country's Ministry of Environmental Protection (Ministry of Environmental Protection, 2016), 78.4% of the nation's cities had air pollution levels that exceeded the Ministry standards. Moreover, a growing number of days per year were characterized as severely polluted. The issue was much more serious in the Beijing-Tianjin-Hebei Region than in the other cities and regions of China (Chen et al., 2017; Gao et al., 2017; Liu et al., 2017; Sun et al., 2013; Wang et al., 2017a,b).

Earlier studies focused on whether tree leaves could dissolve and block air pollutants (Currie and Bass, 2008; Fantozzi et al., 2015; Nowak, 1994, 2002; Rao et al., 2014; Selmi et al., 2016; Smith, 2012; Tallis et al., 2011). Some research revealed that plants were effective in reducing air pollution – not only trees, but also the leaves of shrubs, hedges, or multi-species green roofs, which could filter or deposit gaseous air pollutants via their leaf stoma (Gallagher et al., 2015; Nowak et al., 2006, 2014; Setälä et al., 2013; Tong et al., 2016). Studies showed that by selecting the optimal species of trees, air pollutants could be effectively reduced (Beckett et al., 2000; Morani et al., 2011). In addition, Abhijith and Gokhale (2015) found that selecting trees that were medium-sized and with a higher degree of surface porosity, and planting them in a less dense way, could reduce their blocking effects

Abbreviations: LUR, land use regression; D/S/A, deletion/subtraction/addition machine learning algorithm; NO_2, nitrogen dioxide; $PM_{2.5}$, particulate matter with aero-dynamic diameter ≤2.5 microns; PM_{10}, particulate matter with aero-dynamic diameter ≤10 microns; VOC, volatile organic compounds

* Corresponding author.
E-mail address: jasonsu@berkeley.edu (J.G. Su).

https://doi.org/10.1016/j.ufug.2018.10.013
Received 6 May 2018; Received in revised form 3 September 2018; Accepted 28 October 2018
Available online 31 October 2018
1618-8667/

and help improve air quality. However, no absorption effect could be expected of some plant varieties when air pollution was characterized by high concentrations of volatile organic compounds (VOC) or ozone.

Some studies have identified the associations between air pollution and land cover types including vegetation (Dadvand et al., 2015; Su et al., 2010, 2009, 2011; Villeneuve et al., 2018); however, those studies are largely used for air pollution exposure assessment in an effort to identify the general positive impacts of vegetation on reducing air pollution and improving health. They are not aimed at urban greening applications which focus on location specific strategies to increase vegetation. No studies have been done to identify the amount of reduction in pollutant concentrations in a region that could be attributed to a specific urban greening strategy.

We assume that urban greening strategies generally have a positive impact on reducing local air pollution and the specific reductions can be quantified through the identification of the marginal effects of vegetation in air pollution, through land cover modeling techniques such as land use regression. To fill the gap, we first identified whether vegetation including trees, shrubs and grasslands had a positive effect on reducing air pollution from nitrogen dioxide (NO_2) in Tianjin. Based on the marginal effects of vegetation on reducing air pollution as estimated through land use regression modeling technique, we then identified the specific quality of NO_2 concentration reduction delivered by per unit increases in vegetation cover. Through object-based classification of sub-meter remote sensing data, we identified the current status of urban green cover and the potential for increases in green cover given approaches to urban greening design. The potential increases in green cover from urban greening strategies were then applied to the land use regression modeling results to identify potential reductions in air pollutant concentration. The results of the study can help policy makers and environmental designers adopt effective air pollution reduction policies to improve air quality and protect public health in Tianjin and other urban regions in China.

2. Materials and methods

Using information released by the Tianjin Municipal Government, we identified 23 monitoring stations in the city through their location information (latitude and longitude). Using Google Aerial Maps and Baidu Aerial Maps, we captured an aerial image within a 4 km by 4 km square range surrounding each monitor. The image data were then georeferenced in ArcGIS and imported into e-Cognition™ (Trimble GeoSpatial, Munich, Germany). Each image of a 4 km by 4 km area was segmented into 80,000 ~ 220,000 units of objects. By applying the standard nearest neighborhood classification algorithm, we classified each object into one of 16 land cover types. The classified land cover images were then imported into R statistics analysis for land use regression (LUR) modeling. The bivariate relationships between NO_2 and land cover types and the developed full LUR model were used to identify improvements in air quality given the greening strategies planned by the City.

2.1. Study area

Tianjin (38°34′N ~ 40°15′N, 116°43′E ~ 118°40′E) is situated on the North China Plain, with the Bohai Sea to the east and the Yanshan Mountains to the north (Fig. 1). The city is located at the confluence of the five major tributaries of the Haihe River—the South Canal, the Ziya River, the Daqing River, the Yongding River and the North Canal—that ultimately flows into the Bohai Sea. Tianjin is a primary international shipping node for North China. The climate is temperate semi-humid, and temperature varies noticeably between four seasons. The average annual temperature is around 14 °C and the average precipitation is 550 mm ~ 680 mm, with average wind speed at 2.5 m/s. In 2015, the city had a population of 15,470,000, of which 12,780,000 was classified as urban and 2,690,000 classified as rural. By 2015, Tianjin had a total green area of 28,400 ha, with 8,900 ha in public ownership; 102 parks had been established with a total area of 2,300 ha; and green cover reached 36.4%.

In recent years, air pollution in Tianjin has become severe. According to the *Environmental Quality Report* published by the Tianjin Municipal Government in 2015, the city's major air pollutants are NO_2 (with an annual average concentration of 42 $\mu g/m^3$), particulate matter with aerodynamic diameter $\leq$10 microns (PM_{10}) (annual 116 $\mu g/m^3$), particulate matter with aerodynamic diameter $\leq$2.50 microns ($PM_{2.5}$) (annual 70 $\mu g/m^3$) and ozone (O_3) (annual daily eight hour maximum 142 $\mu g/m^3$). These concentrations are far above the standards set by WHO, which are respectively 40 $\mu g/m^3$, 10 $\mu g/m^3$, 10 $\mu g/m^3$ and 100 $\mu g/m^3$.

2.2. Identification of land cover types

We aimed to identify land cover types that either increase or decrease air pollution. Extensive research has shown that increases in building heights can restrict urban air circulation. Specific building configurations were shown to have a strong impact on the wind flow patterns, influencing the dispersion of pollutants. High-rise buildings in particular create street canyon effects and lead to heightened air pollution levels on the street (Allegrini, 2018; Liu et al., 2011; Peng et al., 2018). Vegetated areas, by contrast, have the potential to purify air and help reduce pollutant concentrations in the urban areas (Currie and Bass, 2008; Janhäll, 2015; Speak et al., 2012; Yang et al., 2008). We also aimed to identify types of land cover that are modifiable, i.e., have potential for planting vegetation. Areas with many high-rise buildings are difficult to augment with green cover. By contrast, bare soil and some public open spaces could be modified to increase vegetative cover and help decrease urban air pollution. Based on these principles, we divided the land cover in the City into five major categories, including buildings, vegetation, roadway/railway, water, and open space. These five categories were further separated into 16 land cover types as listed in Table 1 and further explained in the following paragraphs.

2.2.1. Buildings

Buildings above 10 stories are categorized as high-rise buildings and these high-rise buildings include both residential and commercial buildings. Buildings with less than 10 stories were further classified as residential and public buildings. Industrial buildings refer to factories and some temporary buildings. We specifically created a high-rise building category for the purpose of identifying potential traffic canyon effects, and also because there is limited ability to add vegetation to this type of land use. Another reason for creating a land cover type for high-rise building was due to the fact that it could be effectively identified in remote sensing imagery through its areal shadows (Su et al., 2008).

2.2.2. Vegetation

We classified vegetation into trees/forests, shrublands and grasslands. This classification was based on the impact of plants on air pollutant concentrations (Vieira et al., 2018). Plants may attenuate air pollution because the stomata on their leaves can absorb pollutants (Fellet et al., 2016; Mori et al., 2018; Nowak et al., 2018). Moreover, the overall morphology of plants affects the diffusion of air pollutants (Pandey et al., 2016). Herbaceous plants were included in the grassland category. Woody plants like trees and shrubs differ greatly from their form to their capacity to absorb air pollutants than those of herbaceous plants (Fellet et al., 2016; Nowak et al., 2006). Cultivated lands are part of the urban ecosystem that generates a range of ecosystem services including air purification (Bolund and Hunhammar, 1999). We thus included cultivated lands in the study area as a separate land cover type in the vegetation category.

2.2.3. Roadway and railway

Roads are a very important part of the urban and suburban

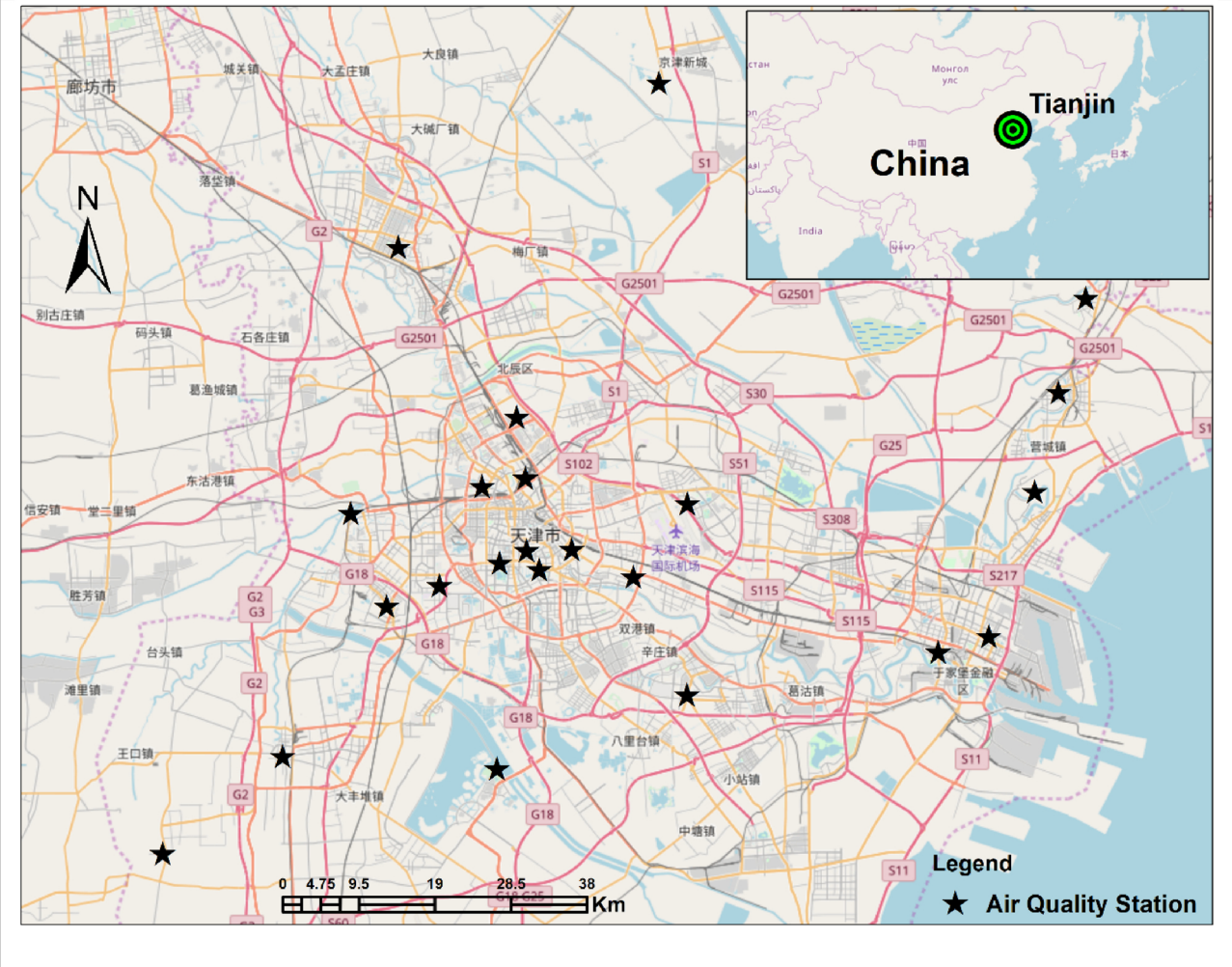

Fig. 1. The City of Tianjian and its air quality monitoring stations.

landscape, with roads and air pollution from vehicles being closely related (Massoli et al., 2012; Su et al., 2015a,b; Su et al., 2010, 2009). Based on the functions of roadways and potential for retrofitting, we used the following classifications: Highways and major roadways are the main sources of traffic-related air pollution and were treated as one class. Roadway overpasses with hardscaped shoulders can be effectively redesigned with vegetation. Local roadways mostly refer to park paths, residential area paths, and the paths in front of buildings. Used for walking, they typically do not contribute to air pollution. Railways are part of the city's public transportation system. Although they contribute to air pollution, due to their special construction standards and forms, land used for rail transportation was identified as a separate category.

Table 1
The list of the land cover categories and types used in the study.

Category	Classification	Description
Buildings	Public building	Public buildings including government agencies, hospitals, schools and universities, and gymnasia.
	Residential building	Housing clustered in residential areas.
	Industrial Building	Industrial construction, such as workshops or factories.
	High-rise building	Buildings with ten stories or more.
Vegetation	Farmland	Paddy fields and croplands.
	Grasslands	Grasslands in city or suburbs.
	Tree plants / Forests	Ligneous plants with a certain height (vines excluded).
Road/Rail	Highways and major roadways	Arterial and secondary roads, freeways, expressways, etc.
	Local roadways	Paths in parks and communities; sidewalks.
	Roadway overpass	Overpasses.
	Railway	Subway and high-speed rail.
Water	Waterbody (non-linear feature)	Water systems of the city (rivers excluded), such as lakes, fountains and reservoirs.
	River (linear feature)	Rivers in the city.
Open Space	Bare soil	Earth, sands and construction sites.
	Urban open space / Public use	Urban square, parking lots
Others	–	Land type unidentified.

2.2.4. Waterbody

Waterbodies are key parts of urban and suburban land cover and have a significant impact on reducing air pollution through their absorption of air pollutant particles through air deposition (Environmental Protection Agency, 2000; Slinn and Slinn, 1980). Also, they do not themselves produce air pollution emissions.

2.2.5. Open space

Open space includes urban public space and bare soil (Stanley et al., 2012). Urban open use space refers to designated areas designed to serve the general public, and includes public activity spaces (e.g., parks and outdoor public recreation and entertainment sites) and parking lots. Bare soil refers to lands that are yet to be developed or are located in the midst of ongoing urban development, such as vacant construction sites and sand lots. Compared to other land cover types, bare soil is more easily modified and is thus central to greening efforts designed to reduce air pollution.

2.3. Land cover classification with e-cognition

We used aerial photos provided by the Baidu aerial maps (http://map.baidu.com/) or Google aerial maps (https://www.google.com/maps) for land cover classification. The highest spatial resolution of the Baidu and Google maps are 0.3 m. Dozens of screenshots were captured for each of the 23 monitoring stations within a 4 km by 4 km square, and mosaicked into a larger image through Photoshop (Adobe, San Jose, CA). The monitoring stations were situated at the center of the corresponding merged images. All the air quality monitoring stations and associated images were calibrated and geo-referenced through ArcGIS (ESRI, Redlands, CA). In geo-referencing, more than six geo-referencing points were used in aligning each of the 23 images to the calibrated images in ArcGIS. These geo-referenced TIF images were then used in an e-Cognition environment for land cover classification.

Urban space consists of many small objects which complicates urban features in spectral responses. Traditional pixel-based spectral algorithms are not sufficient for classifying these spectrally heterogeneous land-cover data (Johansen et al., 2010). In addition, many different urban features might share the same or very similar spectral signals and thus be impossible to classify through pixel-based spectral analysis alone (De Pinho et al., 2012). The availability of high resolution spatial remote sensing data (e.g., sub-meter resolution) gives us the capability to identify and classify those small objects through advanced object-based classification algorithms. E-Cognition (Trimble GeoSpatial, Munich, Germany) is one of the leading object-based remote sensing data processing software platforms successfully used to conduct complex intra-urban land cover classifications (De Pinho et al., 2012; Tehrany et al., 2013; Tijjani Baba, 2015; Xu et al., 2016). In this study, we used e-Cognition to identify objects through a knowledge-based flow chart (De Pinho et al., 2012). First, we applied the fractal net evolution approach (i.e., multi-resolution segmentation algorithm) to generate objects at different scales (e.g., starting from 100 and going smaller by 10) and selected an optimal level for object recognition. Second, we applied a membership function and the nearest neighborhood classifier method to classify the segmented objects into the 16 classes defined in Section 2.5. This approach was applied separately to each of the 23 sites in a 4 km by 4 km square area. Based on the complexity of the land cover surrounding each monitoring site, 80,000 ~ 220,000 image segments were generated. In the process of membership definition, we first classified each segmented object based on their spectral information (i.e., layer values – e.g., green, red, and vegetation index). Spectral information was useful to identify spectrally different objects like vegetation vs. impervious surface vs. water. We then added geometry information into the knowledge base, including extent (e.g., length/width for roads and rivers) and shape (e.g., rectangle for building tops). Merging small size objects into nearest neighborhood and other functions were also used to enhance object classification.

To verify the accuracy of image classification in a 4 km by 4 km scope, we randomly selected 100 classified objects for a detailed assessment, using its sub-meter remote sensing imagery. If a chosen object could not be clearly identified through the areal photo, fieldwork was conducted to assist assessment. In addition, we visually inspected each 4 km by 4 km square area thoroughly to identify potential classification inaccuracy. For the 23 sites, there were 13 urban sites and 10 rural sites. The mean classification accuracy for the urban areas was 75% and the corresponding mean accuracy for the rural areas was 95% (typically agriculture fields). The overall mean accuracy for the 23 sites was 85%.

2.4. Air pollution data and LUR modeling

The LUR methodology seeks to predict pollution concentrations at a given site based on surrounding land use and traffic characteristics. The detailed information on LUR development can be found in Jerrett et al. (2004) and it is briefly described here: LUR uses measured pollution concentrations y at location s as the response variable and land use/cover types x within areas around location s (called buffers) as predictors of the measured concentrations. The method entails the use of least-squares regression modeling to predict pollution surfaces based on pollution monitoring data and existing exogenous independent variables. Air pollution data on NO_2 for Tianjin were collected by the Tianjin Municipal Environmental Protection Bureau for 2015 for the 23 monitoring stations, covering the six urban districts of Heping, Nankai, Hexi, Hebei, Hedong and Hongqiao, as well as the Binhai New Area, Wuqing District and Jizhou District.

To develop a LUR model, we first created buffers of 40 circular area distances with an interval of 50 m (i.e., 0–50 m, 0–100 m, 0–150 m, …, 0–2000 m) around each of the 23 air quality monitoring sites. The buffer statistics for each underlying land cover type were then used in a machine learning LUR modeling approach to identify the more aggregated land cover categories that most accurately predict levels of NO_2 concentrations. The marginal effects of vegetation on reducing air pollution was subsequently identified.

A distance decay curve was first generated to visualize the correlations between air pollution and land cover categories, which were generated through the object-based classification approach. The LUR model was then run through a deletion/substitution/addition (DSA) machine learning algorithm (Beckerman et al., 2013; Su et al., 2015c) using the aggregated nine land cover categories described above. The DSA algorithm is an aggressive model search algorithm which iteratively generates polynomial generalized linear models based on the existing terms in the current 'best' model and the following three steps: (1) a deletion step which removes a term from the model, (2) a substitution step which replaces one term with another, and (3) an addition step which adds a term to the model. The search for the 'best' estimator starts with the base model specified with 'formula': typically the intercept model except when the user requires a number of terms to be forced in the final model. Before searching through the statistical model space of polynomial functions, all data are assigned randomly into v-folds of near equal numbers of observations in each fold. Data in one fold are used for validation while the data in the remaining folds are used for prediction/model training. This process repeats for v-times until all the folds are used for validation. The polynomial within the search space that minimizes the cross-validated risk is selected as the prediction algorithm. In our practice, we limited the predictors to be only on linear terms (the maximum sum of powers in each variable being 1) and disallowed any interaction except corridor by year. The LUR model helped us identify whether the land cover categories and data for the city could effectively predict air pollution NO_2.

2.5. Identification of the effects of the City greening strategies on reducing air pollution reduction

The regression coefficient associated with vegetation in the LUR

model was then used to identify the degree of reduction in air pollutant concentrations when a specific land cover category was retrofitted to increase vegetation coverage. To identify air pollution reduction, we also identified directions of association between individual land cover types and NO_2. These directions indicate whether a land cover contributed to an increase or reduction in air pollution through the direction of association. A positive association (+) indicates contributing to the increase of NO_2 levels while a negative association (-) indicates contributing to the reduction of air pollution and thus improvement in air quality. We also considered the combined effects of multiple greening strategies (e.g., tree top layer + grass understory) in a single place to more effectively reduce air pollution.

For a land cover type that contributed to air pollution (+ sign of association with NO_2), we analyzed the suitability of that category for greening. A land cover category belonging to the "greening" group can generally be modified to mitigate air pollution through retrofitting, including shoulders of highway and major roadways, overpasses, local roadways, and urban open space etc. The "no greening" group includes public buildings, high-rise buildings and railway stations etc. High-rise buildings, for example, due to the traffic canyon effects, might create heightened air pollution levels; however, the prohibitive costs associated with adding green space might preclude this type of land cover from being included in green programs and we thus classified it as "no greening".

There are also differences within the "greening" group, depending on the more detailed land cover type categories. For example, local roadways and urban open spaces are different from major roadways and overpasses in the amount of air pollutants produced and the percentage area available for greening. Further, roadway redesign is not aimed at changing either road width or traffic carrying capacity, but rather to cover the available space with plants based on the current situation, such as mid-road parkways. Similarly, industrial buildings differ from other building types, due to the fact that some factories create air pollution, while others do not, and the strategy for redesign likely depends on specific conditions on the ground.

We used China's national land planning standards to calculate the maximum area and the percentage that could be retrofitted (Table 2). The referenced standards included: Code for Planting Planning and Design of Urban Roads CJJ 75-97, that focuses on planting along roads. The Code for the Design of Urban Green Space GB50420-2007, stresses public design and planting plans of public places. The Code for the Design of Urban Road Engineering CJJ37-2012, pays attention to road planning. The Technical Specification for Planted Roofs, JGJ155-2013, offers preliminary guidance for green rooftops. The Code for the Design of Urban Bridges CJJ11-2011, mainly addresses standards for bridge design. We focused on those land cover types that are modifiable under these standards, which are summarized in Table 2.

3. Results

3.1. E-cognition land cover classification results

We differentiated public, industrial and residential buildings using remote sensing data through guidance provided by the Chinese government on planning indicators for those land uses (MOHURD, 1998, 2010). Public buildings are normally inter-connected to form a big block of buildings, while industrial buildings are typically dispersed and low in height. Residential buildings are typically distributed in parallel blocks, separated from each other in individual elongated polygon shapes, and normally taller than industrial buildings (with more than 10 floors). Residential buildings taller than 27 m are classified as high-rise buildings. As well as shape and layout, shadow information was also used to identify those land uses, i.e., to construct height information. The images were classified through e-Cognition and imported into ArcGIS for further processing. Some of the generated images are shown as follows:

According to Figs. 2 and 3, the urban land cover types are distributed in a relatively orderly fashion: they are separated by grids of roadways, relatively small in size and have multiple land cover types. The road network includes highways, major roadways and local roadways. Open space and green vegetation (e.g., grasslands, street tree stands and forests) are distributed throughout the area. The land devoted to industrial facilities and factories are relatively small and tend to be dispersed among other land cover types. The public buildings are generally bigger in size and concentrated in a specific area. The residential buildings are relatively small in size but constitute the greatest share of the occupied land.

In comparison, land cover types in the rural areas are relatively homogeneous, as shown in Fig. 4, where grasslands, bare soil and farmland make up the bulk of uses. Grasslands and bare soil cover much of the area; areas planted with trees are relatively small and they are distributed mostly along roadways. The public buildings and residential units are relatively concentrated. Buildings are generally lower in height. Table 3 shows the distribution characteristics of each land cover type across the areas surrounding the 23 air quality monitoring stations.

3.2. Model diagnostics: distance decay curves of correlation

Fig. 5 is the visualization of the distance decay curves of Pearson correlations that shows the associations of selected land cover types with air pollution from NO_2.

Table 2
The national standards on greening for 9 land cover categories.

Type	Standard size parameter	Standard greening scale	Max retrofit	retrofit percent
Highway and major roadways (speed > 60 km/h)	3.75 m	Wsb ≥3 m Wsm ≥2.5 m	2*Wsb + Wsm	(2*Wsb + Wsm)/Wr
Highway and major roadways (speed ≤ 60 km/h)	3.5 m	Wsb ≥2 m Wsm ≥2 m	2*Wsb + Wsm	(2*Wsb + Wsm)/Wr
Local roadways	≤3.0 m	≥40%	2.3 m	77%
Roadway overpass	3.75 m	–	2.5 m	67%
Residential building	–	Roof ≥60%	Roof Building elevation	≥90% ≤50%
Industrial building	–	–	Roof	≥90%
Urban Open space	–	25%	All	100%
Grassland	–	–	All	100%
Tree plants	1.2–1.5 m	–	none	0%
Bare soil	–	–	All	100%

Notes: For roadways, the standard size parameter refers to the minimum single lane width. In the standard greening scale column, Wsb refers to road separation barrier between a central roadway and its side roadway while Wsm refers to the middle roadway separation barrier between two main opposite lanes. 2*Wsb + Wsm indicates the maximum greening width: the total width of the two side roadway separation barriers plus the central roadway main separation barrier. Wr is the total roadway width in meters.

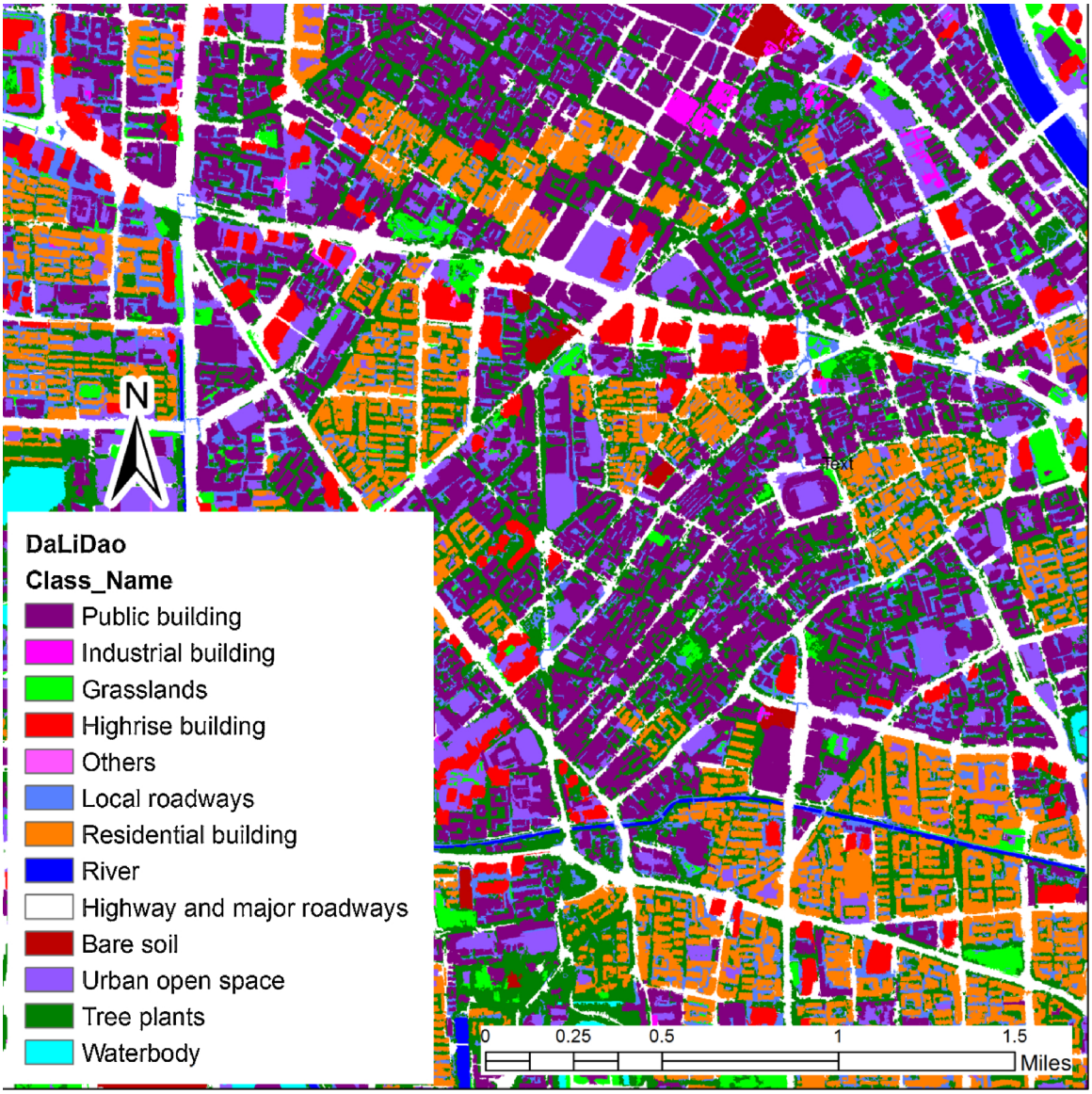

Fig. 2. The land cover classification result in the urban area of Dali Dao.

The distance decay curves of correlation are the incremental relationships in buffer distance between the grouped land cover types and the concentration of NO_2 within a 2 km distance from the 23 monitoring stations, including those from 0 to 50 m, 0–100 m, 0–150 m, …, to 0–2,000 m. It can seen that high way, major road way, local roadway and buildings are positively correlated with NO_2 concentrations while residential, water, vegetation, and industrial land covers are negatively correlated with NO_2.

3.3. Land use regression modeling results

Table 4 displays the LUR modeling results. Overall, the model explained 84% of the variance observed from field air quality monitoring.

3.4. Land cover contribution to air pollution and greening optimization in Tianjin: An example of Qixialu

Through bivariate analysis between a land cover and NO_2, we found that 8 land cover types were associated with increases in NO_2 (Table 5). Among all the land cover types, 6 of them were treated as non-modifiable while another 8 types could be retroffitted to increase greenning.

Based on whether a land cover type can be redesigned to increase vegetation according to the standards promulgated by Chinese planning authorities for greening (Table 2), we calculated the total amount of land that could be redesigned within each area centered around the 23 air quality monitoring stations. Table 6 shows the estimated scale (in hectares) of potential retrofitting that might be accomplished give the land cover types identified in the study, for the Qixialu monitoring station area.

For redesign or retrofitting, we applied the coefficient of the marginal effects of vegetation (including trees/forests, shrubs and grasslands) in our LUR modeling as the optimal strategy for greening. In the area surround monitoring station Qixialu, we found that the total area that could be redesigned is 1372.77 ha or 53.7% of all land area. The LUR modeling coefficients for vegetation are -0.0157 for a buffer distance of m (size = 855.3 ha) and -0.1159 for a buffer distance of 400 m (size = 50.27 ha). Thus total NO_2 reduced based on the marginal effects model would be: 0.0157 * 855.3 * 53.7% + 0.1159 * 50.27 * 53.7% = 10.3 ppb, or 25% of the monitored concentration in 42 ppb in Qixialu area.

4. Discussion and conclusion

In this study, using e-Cognition, we classified land cover in Tianjin,

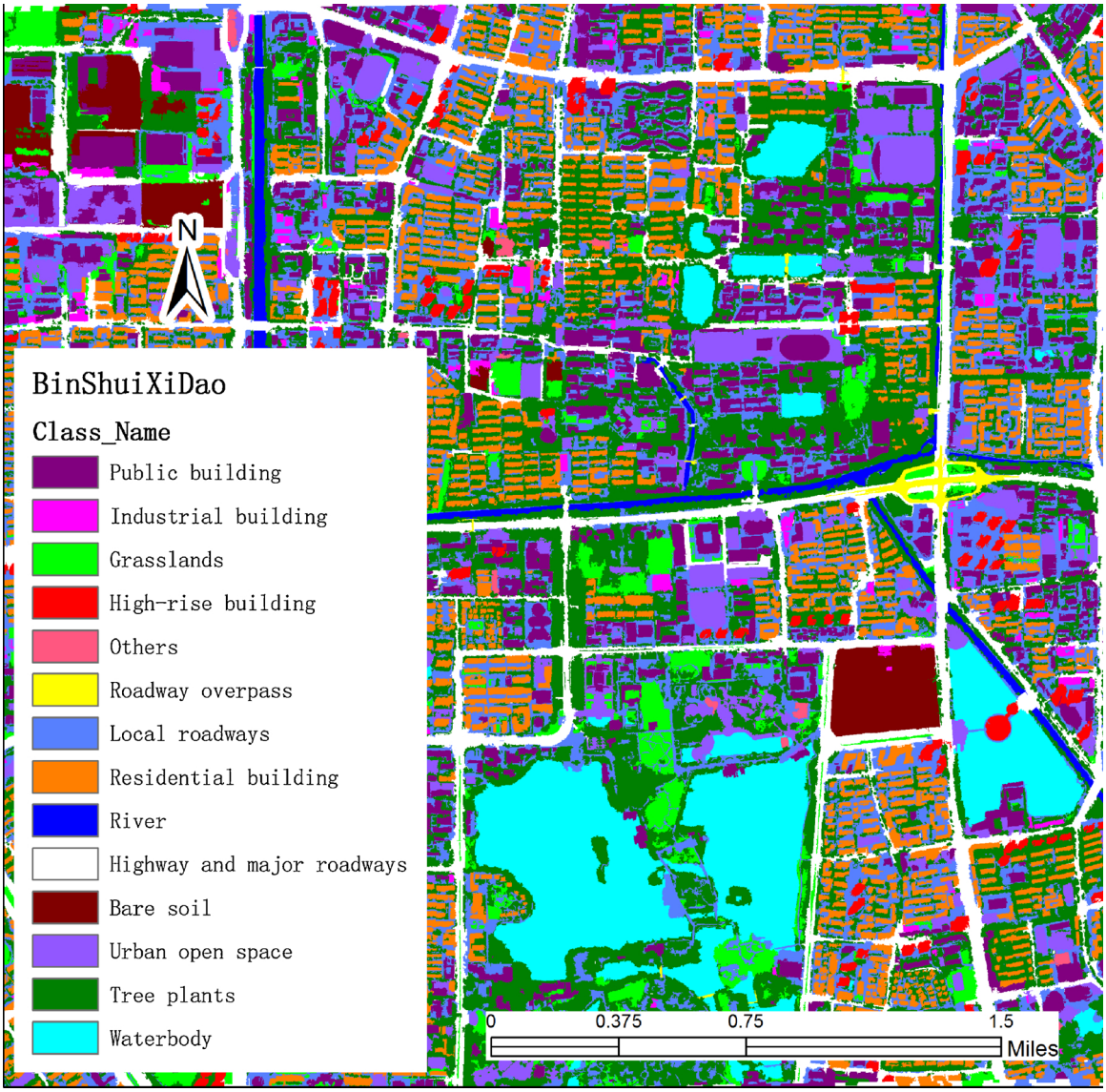

Fig. 3. The land cover classification result in the urban area of Binshui Xi Dao.

within a 4 km by 4 km range of each of the 23 air quality monitoring stations into 16 distinct types with an accuracy of 85%. This accuracy is consistent with other studies that also applied the e-Cognitition software in urban land cover classification (De Pinho et al., 2012; Tehrany et al., 2013; Tijjani Baba, 2015; Xu et al., 2016). In our land cover classification, we did not have surface elevation model or LiDAR (light detection and ranging) data to support object height information. Instead, we used object shadows to adjust for object height information. Though we found some misclassification between grasslands, shrublands and forests, and between residential, industrial and high-rise buildings, application of shadow information helped us retrieve height information of objects, though in a slightly less precise way.

The distance decay curves of correlation and land use regression modeling results are also consistent with previous research findings that vegetated land covers including trees/forests, shrublands and grasslands have positive impacts on reducing air pollutant concentrations, and vegetated lands are the most effective in reducing air pollution (Dadvand et al., 2015; Su et al., 2010, 2009, 2011; Villeneuve et al., 2018) and so should be used as a primary design strategy to combat air pollution where feasible. The land use regression model in our study had an adjusted R^2 of 0.85, relatively higher than most other models and we think it was likely due to the more refined way of characterizing land cover in our study: at a sub-meter resolution in our study vs. 10 m or 30 m resolution in prior studies.

Instead of estimating improvements in air quality at the level of an individual tree, for example, we estimated reduction of air pollution at the land cover level. Further, our analysis aimed to estimate improvements in air quality associated with specific urban greening strategies at a regional level. As such it provides a quantitative method to assess an urban greening strategy and its potential in reducing air pollution levels.

In regard to urban greening, we identified some exemplary models that are worth further examination and implementation. For greening residential land uses, the ACROS building design and the Garden House design by Müller Sigrist, Emilio Ambasz and Wilkinson (Currie and Bass, 2008; Li et al., 2010; Yang et al., 2008) could be used for effective urban greening. For highways and major roadways, local roadways, and roadway overpasses, urban designers should take advantage of middle lanes and parkways in order to increase the extent of vegetation coverage. Precedents for such strategies include the Buffalo Niagara Medical Campus Streetscape, High Line Park in New York, Pancras Square in London, Vancouver's Land Bridge, and Seoullo 7017 Skygarden in Seoul (Finch and Morfei, 2010; Hynd and Berglund, 2017). Most urban open space, grassland and bare soil have some grass/shrub coverage but

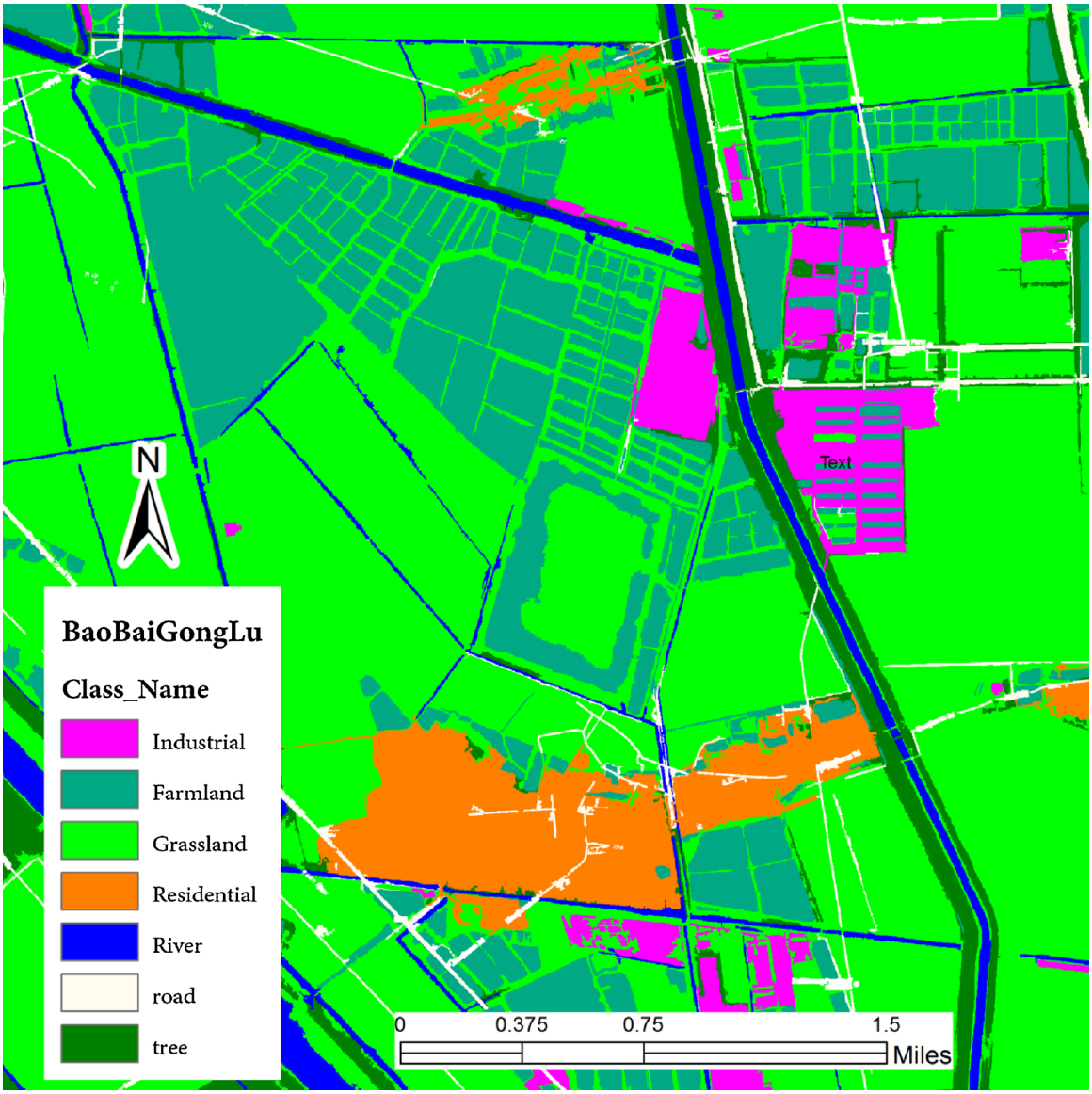

Fig. 4. The land cover classification result in the urban area of Baobai Gong Lu.

Table 3
The descriptive statistics on the land cover categories surrounding the 23 air quality monitoring stations in Tianjin, China.

	Total (ha)	Max (ha)	Min (ha)	Mean (ha)
Public building	10153.3	2110.11	55.19	534.38
Industrial building	11203.63	2304.93	10.39	487.11
Residential building	13260.09	2731.28	30.16	576.53
Farmland	3881.855	1089.36	0.00	258.79
Grasslands	55463.94	12595.36	70.53	2411.48
Highway and major roadways	15756.4	3065.08	56.69	685.06
Waterbody	5037.557	1229.98	1.92	228.98
River (linear feature)	6340.967	1425.61	11.01	288.23
Local roadways	21034.5	6986.08	39.68	956.11
Urban open space	9031.895	2306.37	14.96	410.54
High-rise building	3320.218	1275.24	18.77	174.75
Others	1112.504	447.34	0.82	55.63
Tree plants	19793.49	4342.24	46.30	860.59
Bare soil	9027.954	2110.11	55.19	534.38
Roadway overpass	712.5062	2304.93	10.39	487.11

could also be enhanced with trees to further increase vegetation cover. Here, design precedents to consider include the Tianjin Duishan Park, Hamilton Bayfront Park, Amsterdam Westergasfabriek, and Circular Park (Edge and Hill, 2005; Koekebakker and Joseph, 2003).

Despite its utility, we also realize that our study has certain limitations. The analytic method requires air quality monitoring that covers various land cover types in an urban area. Such an approach is clearly a challenge to cities without an air quality monitoring network and thus no detailed air quality data. Tianjin's air quality monitoring network included 23 sites across various land use and land cover types; however, future efforts should include more air quality monitoring stations (e.g., more than 40 sites) to make the LUR modeling results more stable. Further, our study requires detailed land cover classification through an object-based classification algorithm. Some land use planning and urban greening institutes may not have the resources to conduct such complex analytic tasks. We also envision difficulties in changing urban land cover patterns. Although we can build a green roof or implement vertical greening technologies for residential and industrial buildings, the cost may be prohibitive, and there are practical issues around waterproofing and drainage technology. Moreover, large-scale treatment of air pollution through greening strategies may disrupt everyday life and urban economic development, despite its long-run benefits to public health and urban vitality. Thus, practical greening programs will need to rely on landscape architects, urban designers and

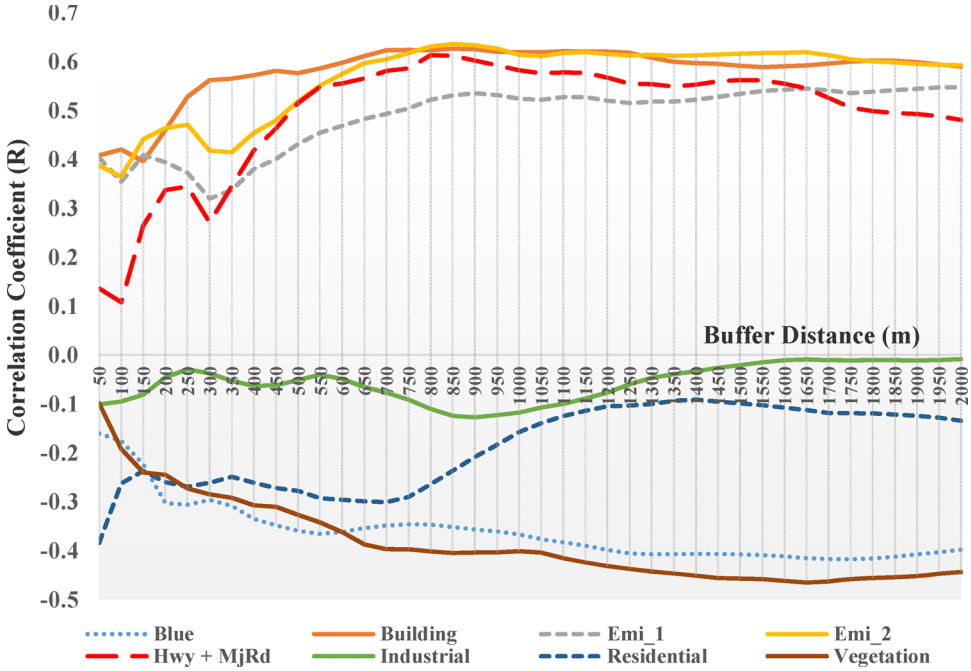

Fig. 5. The correlation distance decay curves between land cover types and measured NO_2 for buffers 50–2000 m. Blue represents farmland, waterbodies, and rivers; Emi_1 represents roadways (highway and major roadways), overpassses, urban open space (parks and parking lots), and railways; Emi_2 stands for Emi_1 plus local roadways; Hwy + MjRd stands for highways and major roadways; and lastly, vegetation represents grassland, trees/forests and shrubland (For interpretation of the references to colour in this figure legend, the reader is referred to the web version of this article).

Table 4
Land use regression modeling results for Tianjin, China.

Predictor	Estimate	Std. Error	t value	Pr (> |t|)
(Intercept)	51.5110	2.3090	22.31	0.000
Highway and major roadway (ha) (800 m)	0.1332	0.0434	3.07	0.007
Vegetation (ha) (1650 m)	−0.0157	0.0039	−4.07	0.001
Residential building (ha) (2000 m)	−0.0313	0.0045	−6.87	0.000
Industrial building (ha) (900 m)	−0.0437	0.0133	−3.28	0.004
Vegetation (ha) (400 m)	−0.1159	0.0543	−2.13	0.048

Note: ha is the area in hectares for with a buffer distance (second parenthesis) of a specific land cover type.

Table 5
The effect of land cover types on air pollution and associated potential for greening.

	Relation to Air Pollution	Potential for Greening
Public building	↑ (increase)	No
Residential building	↓ (reduce)	Yes
Industrial building	↑	–
High-rise building	↑	No
Farmland	↓	No
Grasslands	↓	Yes
Tree plants	↓	Yes
Bare soil	↓	Yes
Highway and major roadways	↑	Yes
Local roadways	↑	Yes
Urban open space	↑	Yes
Roadway overpass	↑	Yes
Railway	↑	No
Waterbody (non-linear)	↓	No
River (linear feature)	↓	No
Others	–	–

engineers to develop not only building-level but also city-level greening programs and related green infrastructural interventions.

In summary, this is the first study to apply a machine learning LUR modeling technique to identify the marginal effects of vegetation on reducing air pollution and then use those relationships to quantify the potential improvements in air quality associated with urban greening

Table 6
Estimated hectares of land available for green redesign, Qixialu monitoring station.

Qixialu	Pixel Count	hectare	Retrofit percent (max)	Retrofit area (ha)
Public building	1730614	174.1	–	–
Industrial building	599281	60.29	Roof ≥90%	6.02
Residential building	3049764	306.81	Roof ≥90%	15.34
Farmland	367983	37.02	–	–
Grasslands	5125279	515.60	100%	515.60
Highway and major roadways	2130208	214.30	7.5%	16.07
Waterbody	99375	9.997	–	–
River	1312936	132.08	–	–
Local roadways	3319336	333.93	77%	257.13
Urban open space	2394060	240.84	100%	240.84
High-rise building	888664	89.40	–	–
Others	116195	11.69	–	–
Tree plants	2534057	254.93	0%	0
Bare soil	3008164	302.62	100%	302.62
Roadway overpass	284082	28.58	67%	19.15

strategies. Our approach demonstrated that LUR modeling techniques could be used in urban environmental design to help policy makers and city planners improve air quality and protect public health.

Acknowledgement

The project was funded by Tianjin University, Tianjin, China, for Ying Guo's visiting scholar research at the University of California, Berkeley.

References

Abhijith, K., Gokhale, S., 2015. Passive control potentials of trees and on-street parked cars in reduction of air pollution exposure in urban street canyons. Environ. Pollut. 204, 99–108.
Allegrini, J., 2018. A wind tunnel study on three-dimensional buoyant flows in street canyons with different roof shapes and building lengths. Build. Environ. 143, 71–88.
Beckerman, B.S., Jerrett, M., Serre, M., Martin, R.V., Lee, S.-J., van Donkelaar, A., Ross, Z., Su, J., Burnett, R.T., 2013. A hybrid approach to estimating national scale spatiotemporal variability of PM2.5 in the contiguous United States. Environ. Sci. Technol. 47, 7233–7241.

Beckett, K.P., Freer Smith, P., Taylor, G., 2000. Effective tree species for local air quality management. Arboricultural J. 26, 12–19.
Bentayeb, M., Wagner, V., Stempfelet, M., Zins, M., Goldberg, M., Pascal, M., Larrieu, S., Beaudeau, P., Cassadou, S., Eilstein, D., 2015. Association between long-term exposure to air pollution and mortality in France: A 25-year follow-up study. Environ. Int. 85, 5–14.
Bolund, P., Hunhammar, S., 1999. Ecosystem services in urban areas. Ecol. Econ. 29, 293–301.
Chen, X., Zhang, L.-w., Huang, J.-j., Song, F.-j., Zhang, L.-p., Qian, Z.-m., Trevathan, E., Mao, H.-j., Han, B., Vaughn, M., 2016. Long-term exposure to urban air pollution and lung cancer mortality: a 12-year cohort study in Northern China. Sci. Total Environ. 571, 855–861.
Chen, L., Shi, M., Li, S., Gao, S., Zhang, H., Sun, Y., Mao, J., Bai, Z., Wang, Z., Zhou, J., 2017. Quantifying public health benefits of environmental strategy of PM2. 5 air quality management in Beijing–Tianjin–Hebei region, China. J. Environ. Sci. 57, 33–40.
Currie, B.A., Bass, B., 2008. Estimates of air pollution mitigation with green plants and green roofs using the UFORE model. Urban Ecosyst. 11, 409–422.
Dadvand, P., Rivas, I., Basagana, X., Alvarez-Pedrerol, M., Su, J., De Castro Pascual, M., Amato, F., Jerret, M., Querol, X., Sunyer, J., Nieuwenhuijsen, M.J., 2015. The association between greenness and traffic-related air pollution at schools. Sci Total. Environ. 523, 59–63.
De Pinho, C.M.D., Fonseca, L.M.G., Korting, T.S., De Almeida, C.M., Kux, H.J.H., 2012. Land-cover classification of an intra-urban environment using high-resolution images and object-based image analysis. Int. J. Remote. Sens. 33, 5973–5995.
Edge, T.A., Hill, S., 2005. Occurrence of antibiotic resistance in Escherichia coli from surface waters and fecal pollution sources near Hamilton. Ont. Canadian J. Microbiol. 51, 501–505.
Environmental Protection Agency, U., 2000. Deposition of Air Pollutants to the Great Waters: Third Report to Congress. Accessed on 08/25/2018 from. . https://nepis.epa.gov/Exe/ZyPURL.cgi?Dockey=00002VG1.TXT.
Fantozzi, F., Monaci, F., Blanusa, T., Bargagli, R., 2015. Spatio-temporal variations of ozone and nitrogen dioxide concentrations under urban trees and in a nearby open area. Urban Climate 12, 119–127.
Fellet, G., Pošćić, F., Licen, S., Marchiol, L., Musetti, R., Tolloi, A., Barbieri, P., Zerbi, G., 2016. PAHs accumulation on leaves of six evergreen urban shrubs: a field experiment. Atmos. Pollut. Res. 7, 915–924.
Finch, S., Morfei, M., 2010. Regional Trail Spines and Bikeway Networks: A Priority Strategy for Greening Streets and Highways, Green Streets and Highways 2010: An Interactive Conference on the State of the Art and How to Achieve Sustainable Outcomes. pp. 116–134.
Gallagher, J., Baldauf, R., Fuller, C.H., Kumar, P., Gill, L.W., McNabola, A., 2015. Passive methods for improving air quality in the built environment: a review of porous and solid barriers. Atmos. Environ. 120, 61–70.
Gao, J.-F., Fan, X.-Y., Li, H.-Y., Pan, K.-L., 2017. Airborne bacterial communities of PM2. 5 in Beijing-Tianjin-hebei megalopolis, China as revealed By illumina MiSeq sequencing: A case study. Aerosol Air Quality Res. 17, 788–798 (i.
Guan, W.-J., Zheng, X.-Y., Chung, K.F., Zhong, N.-S., 2016. Impact of air pollution on the burden of chronic respiratory diseases in China: time for urgent action. Lancet 388, 1939–1951.
He, G., Fan, M., Zhou, M., 2016. The effect of air pollution on mortality in China: evidence from the 2008 Beijing olympic games. J. Environ. Econ. Manage. 79, 18–39.
Hynd, A.M., Berglund, A., 2017. Conceiving dream cities: the development of homeless habitats around Seoul station. In: The 2nd Conference for Human Rights Leaders of the Next Generation. March 31, Korea University, Seoul, Korea.
Janhäll, S., 2015. Review on urban vegetation and particle air pollution – deposition and dispersion. Atmos. Environ. 105, 130–137.
Jerrett, M., Arain, A., Kanaroglou, P., Beckerman, B., Potoglou, D., Sahsuvaroglu, T., Morrison, J., Giovis, C., 2004. A review and evaluation of intraurban air pollution exposure models. J Expo. Anal. Env. Epid. 15, 185.
Johansen, K., Arroyo, L.A., Phinn, S., Witte, C., 2010. Comparison of geo-object based and pixel-based change detection of riparian environments using High spatial Resolution multi-spectral imagery. Photogramm. Eng. Rem. S 76, 123–136.
Koekebakker, O., Joseph, V.J., 2003. Westergasfabriek Culture Park: Transformation of a Former Industrial Site in Amsterdam. NAi Publishers.
Li, M., 2016. Haze pollution control strategies in China from the perspective of energy conservation and emission reduction. Nat. Environ. Pollut. Technol. 15, 887.
Li, J.-f., Wai, O.W., Li, Y., Zhan, J.-m., Ho, Y.A., Li, J., Lam, E., 2010. Effect of green roof on ambient CO 2 concentration. Build. Environ. 45, 2644–2651.
Liu, X.P., Niu, J.L., Kwok, K.C., 2011. Analysis of concentration fluctuations in gas dispersion around high-rise building for different incident wind directions. J. Hazard. Mater. 192, 1623–1632.
Liu, B.-C., Binaykia, A., Chang, P.-C., Tiwari, M.K., Tsao, C.-C., 2017. Urban air quality forecasting based on multi-dimensional collaborative support vector regression (SVR): a case study of Beijing-Tianjin-Shijiazhuang. PLoS One 12, e0179763.
Ma, Y., Zhang, H., Zhao, Y., Zhou, J., Yang, S., Zheng, X., Wang, S., 2017. Short-term effects of air pollution on daily hospital admissions for cardiovascular diseases in western China. Environ. Sci. Pollut. Res. 1–9.
Massoli, P., Fortner, E.C., Canagaratna, M.R., Williams, L.R., Zhang, Q., Sun, Y., Schwab, J.J., Trimborn, A., Onasch, T.B., Demerjian, K.L., Kolb, C.E., Worsnop, D.R., Jayne, J.T., 2012. Pollution gradients and chemical characterization of particulate matter from vehicular traffic near Major roadways: results from the 2009 queens College air quality study in NYC. Aerosol. Sci. Tech. 46, 1201–1218.
Ministry of Environmental Protection, 2016. Report on the State of the Environment in China. Accessed on May 6, 2018 from http://english.sepa.gov.cn/Resources/Reports/soe/ReportSOE/201709/P020170929573904364594.pdf.
MOHURD, A., 1998. Standard for Basic Terminology of Urban Planning. pp. 7.
Mohurd, A., 2010. Code for Classification of Urban Land Use and Planning Standards of Development Land. pp. 4–13.
Morani, A., Nowak, D.J., Hirabayashi, S., Calfapietra, C., 2011. How to select the best tree planting locations to enhance air pollution removal in the MillionTreesNYC initiative. Environ. Pollut. 159, 1040–1047.
Mori, J., Fini, A., Galimberti, M., Ginepro, M., Burchi, G., Massa, D., Ferrini, F., 2018. Air pollution deposition on a roadside vegetation barrier in a Mediterranean environment: combined effect of evergreen shrub species and planting density. Sci. Total Environ. 643, 725–737.
Nowak, D.J., 1994. Air pollution removal by Chicago's urban forest. Chicago'S Urban Forest Ecosystem: Results of the Chicago Urban Forest Climate Project. pp. 63–81.
Nowak, D.J., 2002. The Effects of Urban Trees on Air Quality. USDA Forest Service, pp. 96–102.
Nowak, D.J., Crane, D.E., Stevens, J.C., 2006. Air pollution removal by urban trees and shrubs in the United States. Urban For. Urban Green 4, 115–123.
Nowak, D.J., Hirabayashi, S., Bodine, A., Greenfield, E., 2014. Tree and forest effects on air quality and human health in the United States. Environ. Pollut. 193, 119–129.
Nowak, D.J., Hirabayashi, S., Doyle, M., McGovern, M., Pasher, J., 2018. Air pollution removal by urban forests in Canada and its effect on air quality and human health. Urban For. Urban Green 29, 40–48.
Pandey, A.K., Pandey, M., Tripathi, B.D., 2016. Assessment of air pollution tolerance index of some plants to develop vertical gardens near street canyons of a polluted tropical city. Ecotoxicol. Environ. Saf. 134, 358–364.
Peng, L., Liu, J.-P., Wang, Y., Chan, P.-w., Lee, T.-c., Peng, F., Wong, M.-s., Li, Y., 2018. Wind weakening in a dense high-rise city due to over nearly five decades of urbanization. Build. Environ. 138, 207–220.
Rao, M., George, L.A., Rosenstiel, T.N., Shandas, V., Dinno, A., 2014. Assessing the relationship among urban trees, nitrogen dioxide, and respiratory health. Environ. Pollut. 194, 96–104.
Selmi, W., Weber, C., Rivière, E., Blond, N., Mehdi, L., Nowak, D., 2016. Air pollution removal by trees in public green spaces in Strasbourg city, France. Urban For. Urban Green 17, 192–201.
Setälä, H., Viippola, V., Rantalainen, A.-L., Pennanen, A., Yli-Pelkonen, V., 2013. Does urban vegetation mitigate air pollution in northern conditions? Environ. Pollut. 183, 104–112.
Shostya, A., 2016. Ambient air pollution in China: predicting a turning point. Int. Adv. Econ. Res. 22, 295–307.
Slinn, S.A., Slinn, W.G.N., 1980. Predictions for particle deposition on natural-waters. Atmos. Environ. 14, 1013–1016.
Smith, W.H., 2012. Air Pollution and Forests: Interactions Between Air Contaminants and Forest Ecosystems. Springer Science & Business Media.
Song, C., Wu, L., Xie, Y., He, J., Chen, X., Wang, T., Lin, Y., Jin, T., Wang, A., Liu, Y., 2017. Air pollution in China: status and spatiotemporal variations. Environ. Pollut. 227, 334–347.
Speak, A.F., Rothwell, J.J., Lindley, S.J., Smith, C.L., 2012. Urban particulate pollution reduction by four species of green roof vegetation in a UK city. Atmos. Environ. 61, 283–293.
Stanley, B., Stark, B.L., Johnston, K., E Smith, M., 2012. Urban Open Spaces in Historical Perspective: A Transdisciplinary Typology and Analysis.
Su, J.G., Brauer, M., Buzzelli, M., 2008. Estimating urban morphometry at the neighborhood scale for improvement in modeling long-term average air pollution concentrations. Atmos. Environ. 42, 7884–7893.
Su, J.G., Jerrett, M., Beckerman, B., Wilhelm, M., Ghosh, J.K., Ritz, B., 2009. Predicting traffic-related air pollution in Los Angeles using a distance decay regression selection strategy. Environ. Res. 109, 657–670.
Su, J.G., Jerrett, M., Beckerman, B., Verma, D., Arain, M.A., Kanaroglou, P., Stieb, D., Finkelstein, M., Brook, J., 2010. A land use regression model for predicting ambient volatile organic compound concentrations in Toronto, Canada. Atmos. Environ. 44, 3529–3537.
Su, J.G., Jerrett, M., de Nazelle, A., Wolch, J., 2011. Does exposure to air pollution in urban parks have socioeconomic, racial or ethnic gradients? Environ. Res. 111, 319–328.
Su, J.G., Apte, J.S., Lipsitt, J., Garcia-Gonzales, D.A., Beckerman, B.S., de Nazelle, A., Texcalac-Sangrador, J.L., Jerrett, M., 2015a. Populations potentially exposed to traffic-related air pollution in seven world cities. Environ. Int. 78, 82–89.
Su, J.G., Hopke, P.K., Tian, Y.L., Baldwin, N., Thurston, S.W., Evans, K., Rich, D.Q., 2015b. Modeling particulate matter concentrations measured through mobile monitoring in a deletion/substitution/addition approach. Atmos. Environ. 122, 477–483.
Su, J.G., Jerrett, M., Meng, Y.Y., Pickett, M., Ritz, B., 2015c. Integrating smart-phone based momentary location tracking with fixed site air quality monitoring for personal exposure assessment. Sci. Total. Environ. 506, 518–526.
Sun, Y., Wang, Z., Fu, P., Yang, T., Jiang, Q., Dong, H., Li, J., Jia, J., 2013. Aerosol composition, sources and processes during wintertime in Beijing, China. Atmos. Chem. Phys. 13, 4577–4592.
Tallis, M., Taylor, G., Sinnett, D., Freer-Smith, P., 2011. Estimating the removal of atmospheric particulate pollution by the urban tree canopy of London, under current and future environments. Landsc. Urban Plan. 103, 129–138.
Tehrany, M.S., Pradhan, B., Jebur, M.N., 2013. Remote sensing data reveals eco-environmental changes in urban areas of Klang Valley, Malaysia: contribution from object based analysis. J. Indian Soc. Remot. 41, 981–991.
Tijjani Baba, S., 2015. Comparison and Analysis of the Pixel-Based and Object-Oriented Methods for Land Cover Classification With ETM+ Data.
Tong, Z., Baldauf, R.W., Isakov, V., Deshmukh, P., Zhang, K.M., 2016. Roadside vegetation barrier designs to mitigate near-road air pollution impacts. Sci. Total Environ. 541, 920–927.

Turner, M.C., Krewski, D., Diver, W.R., Pope III, C.A., Burnett, R.T., Jerrett, M., Marshall, J.D., Gapstur, S.M., 2017. Ambient air pollution and cancer mortality in the cancer prevention study II. Environ. Health Perspect. 125, 087013.

Vieira, J., Matos, P., Mexia, T., Silva, P., Lopes, N., Freitas, C., Correia, O., Santos-Reis, M., Branquinho, C., Pinho, P., 2018. Green spaces are not all the same for the provision of air purification and climate regulation services: the case of urban parks. Environ. Res. 160, 306–313.

Villeneuve, P.J., Jerrett, M., Brenner, D., Su, J., Chen, H., McLaughlin, J.R., 2014. A case-control study of long-term exposure to ambient volatile organic compounds and lung cancer in Toronto, Ontario, Canada. Am. J. Epidemiol. 179, 443–451.

Villeneuve, P.J., Jerrett, M., Su, J.G., Weichenthal, S., Sandler, D.P., 2018. Association of residential greenness with obesity and physical activity in a US cohort of women. Environ. Res. 160, 372–384.

Wang, C., Huang, X.-F., Zhu, Q., Cao, L.-M., Zhang, B., He, L.-Y., 2017a. Differentiating local and regional sources of Chinese urban air pollution based on the effect of the Spring festival. Atmos. Chem. Phys. 17, 9103–9114.

Wang, Y., Liu, H., Mao, G., Zuo, J., Ma, J., 2017b. Inter-regional and sectoral linkage analysis of air pollution in Beijing–Tianjin–Hebei (Jing-Jin-Ji) urban agglomeration of China. J. Clean. Prod. 165, 1436–1444.

World Health Organization, 2016. Ambient Air Pollution: A Global Assessment of Exposure and Burden of Disease. Accessed on 10/23/2017 @. http://apps.who.int/iris/bitstream/10665/250141/1/9789241511353-eng.pdf.

Xu, Q.Q., Liu, Z.J., Yang, M.Z., Ren, H.C., Song, C., Li, F.F., 2016. A hybrid change detection analysis using high-resolution remote sensing image. IOP Conf. Ser. Earth Environ. 46.

Yang, J., Yu, Q., Gong, P., 2008. Quantifying air pollution removal by green roofs in Chicago. Atmos. Environ. 42, 7266–7273.